Investigation of Carboxylic Acid Isosteres for Inhibition of the Human SIRT5 Lysine Deacylase Enzyme

Nima Rajabi,[†] Alexander L. Nielsen,[‡,#] Tobias N. Hansen,[#] Huy T. Nguyen,[§] Michael Bæk, Julie. E. Bolding, Oskar Ø. Bahlke, Sylvester E. G. Petersen, Christian R. O. Bartling, Kristian Strømgaard, and Christian A. Olsen**

Center for Biopharmaceuticals & Department of Drug Design and Pharmacology, Faculty of Health and Medical Sciences, University of Copenhagen, Universitetsparken 2, DK-2100, Copenhagen, Denmark.

[†]*Present address: Red Glead Discovery, 223 63, Lund, Sweden.*

[‡]*Present address: Institute of Chemical Sciences and Engineering, Ecole Polytechnique Fédérale de Lausanne (EPFL), CH-1015, Lausanne, Switzerland.*

[§]*Present address: School of Chemistry, University of Sydney, NSW 2006, Australia.*

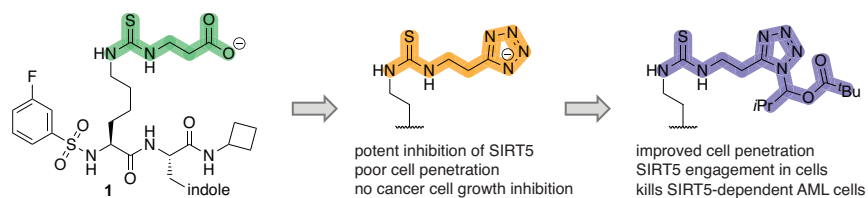[#]*These authors contributed equally to the work*

**Corresponding author:* cao@sund.ku.dk

Abstract (150 words)

Sirtuin 5 (SIRT5) is a protein lysine deacylase enzyme that regulates diverse biology by hydrolyzing ε-N-carboxyacyllysine posttranslational modifications in the cell. Inhibition of SIRT5 has been linked to potential treatment of several cancers but potent compounds with activity in cells have been lacking. Here we developed mechanism-based inhibitors that incorporate isosteres of a carboxylic acid residue that is important for high-affinity binding to the enzyme active site. By masking of the tetrazole moiety of the most potent candidate from our initial SAR study, we achieved potent and cytoselective growth inhibition for the treatment of SIRT5-dependent leukemic cancer cell lines in culture. Thus, we provide an efficient, cellularly active small molecule that targets SIRT5, which can help elucidate its function and potential as a future drug target. This work shows that masked biosisosteres of carboxylic acids are viable chemical motifs for the development of inhibitors that target mitochondrial enzymes, which may have applications beyond the sirtuin field.

Keywords: Sirtuins, SIRT5, bioisosteres, prodrugs, enzyme inhibitors

TOC graphic (11×2.5 cm)

potent inhibition of SIRT5
poor cell penetration
no cancer cell growth inhibition

improved cell penetration
SIRT5 engagement in cells
kills SIRT5-dependent AML cells

Introduction

The sirtuins are NAD^+-dependent lysine deacylases, which are conserved across all domains of life. Humans express seven isoforms (SIRT1–7), which are involved in the regulation of important biological pathways such as gene expression and metabolism.[1,2] All sirtuins share a fundamental NAD^+-dependent hydrolytic mechanism but the seven isoforms differ in substrate specificity, which is particularly manifested with respect to their recognition of various ε-*N*-acyllysine functionalities. These differences have been elucidated through substrate screening efforts and numerous X-ray co-crystal crystal structures.[3–6] Sirtuins 1–3 and 6 have exhibited preference for aliphatic acyl chains of different length ranging from ε-*N*-acetyllysine (Kac) to ε-*N*-myristoyllysine (Kmyr),[7–9] which is also reflected by hydrophobic binding pockets.[10–13] Moreover, SIRT1–3 has recently been reported to cleave both the D and L stereoisomers of ε-*N*-lactyllysine (Klac);[14,15] albeit, with lower efficiency than the zinc-dependent HDACs 1–3.[15] Sirtuin 4 has been reported to cleave negatively charged modifications, such as ε-*N*-methylglutaconyllysine (Kmgc) and ε-*N*-(3-hydroxy-3-methylglutaryl)lysine (Khmg),[16,17] as well as ε-*N*-lipoyllysine (Klip) and ε-*N*-biotinyllysine (Kbio).[18] Sirtuin 7 has been reported to cleave long chain acyl groups[19,20] and ε-*N*-glutaryllysine (Kglut),[21] and has been reported to be activated by oligonucleotides.[19,22] The sirtuin with the most distinct structural features, governing substrate recognition in its binding pocket is SIRT5, which contains a Tyr102–Arg105 motif that interact with carboxylates in the substrate. As such, SIRT5 has a preference for acidic posttranslational modifications (PTMs) such as ε-*N*-malonyllysine (Kmal), ε-*N*-succinyllysine (Ksuc), and ε-*N*-glutaryllysine (Kglut).[23–25]

Sirtuin 5 is one of three sirtuins (SIRT3–5) that primarily localize to the mitochondria and several mitochondrial proteins are subjected to SIRT5-mediated deacylation.[26–28] For example, SIRT5 rescues the activity of superoxide dismutase 1 (SOD1) by desuccinylation of modified lysine residues to (1) eliminate reactive oxygen species (ROS) generated during oxidative phosphorylation,[29] (2) protect mitochondrial autophagy under starvation,[30] and (3) reduce macrophage-induced inflammation *in vivo*.[31] Furthermore, SIRT5 has been identified in both the cytosol and nucleus, where it is proposed to desuccinylate modified proteins as well.[26] With an increasing number of reports implicating SIRT5 in pathogenesis, including as a liability in various cancers,[32–41] there is a growing need for effective inhibitors that can be applied in living cells.

Inspired by the substrate specificity of SIRT5,[24,42,43] we and others have reported on mechanism-based inhibitors of SIRT5 that contained carboxylate moieties to mimic the preferred substrate of the enzyme.[44],[45–48] Recently, one of our lead compounds (**1**) was then developed into an ethyl ester prodrug (**1-Et**), which was shown to exhibit efficacy against cultured cancer cells (see Figure 1 for structures).[41] These investigations indicated that the carboxylate moiety of the parent compounds was a major liability with respect to cellular entry, because compounds could gain activity in cells upon masking of this functional group, while the simple ester prodrugs are likely hydrolyzed by various esterases once inside the cell. In medicinal chemistry, an alternative strategy to prodrug formation is the use of bioisosteres, which may mimic the interactions of a certain functional group (here

3

a carboxylate), while imposing improved properties with respect to for example degradation, clearance, and cellular entry. Here, we report a substantial structure–activity relationship (SAR) study of a series of inhibitors, containing isosteres of the carboxylic acid moiety that is important for ligand affinity to the SIRT5 active site, which produced inhibitors that were equipotent or slightly more potent than the parent compound. Cell penetration was then assessed by applying the chloroalkane penetration assay (CAPA)[49,50] and target engagement was evaluated by cellular thermal shift assays, revealing similar behavior of the carboxylic acid-containing parent compound and its most potent new analogs. Thus, we show that masking of the tetrazole moiety of the most potent compound can provide improved target engagement in cells to furnish a cellularly active tool compound. Finally, we demonstrate that cultured SIRT5-dependent cancer cells (e.g., SKM-1) are susceptible to the masked tetrazole compounds at concentrations where limited effect is observed against HEK293T cells.

Results

Structure–activity relationship study. With compound **1** as the starting point, we first directed our attention to investigating whether bioisosteres of its carboxylic acid moiety could be developed that would retain potency against SIRT5. Inspired by previously reported isosteres, we synthesized the series of compounds **2**–**27**, containing a variety of different functional groups with varying ability to form hydrogen bonds and engage in electrostatic interactions with the target. The inhibitory potencies of all compounds against the lysine deglutarylase activity of recombinant SIRT5 were then determined (Figure 1A; for syntheses see Supporting Schemes S2–S13). The aliphatic analog **2** and alcohol-containing analog **3** did not show substantial inhibition of SIRT5 even at 100 μM. The amide analog **4**, on the other hand, exhibited some potency, but with an IC$_{50}$ value two orders of magnitude higher than for compound **1**.[51] The sulfonates (**5**, **6**), sulfonamide (**7**), phosphonate (**8**), boronates (**9**–**11**), and fluorophenols (**12,13**) all exhibited poor inhibition of SIRT5. Among the series of heterocycles in our array of compounds (**14**–**26**), on the other hand, the 1,2,4-oxadiazol-5(4*H*)-one (**16**) and the tetrazole (**24**) exhibited similar IC$_{50}$ values to the parent compound (**1**), while the 2-hydroxy-isoxazole (**22**) also had a sub-micromolar IC$_{50}$ value (Figure 1). Finally, substituting the carboxylic acid for a hydroxamic acid (**27**) resulted in substantial loss of potency. Interestingly, the pK_a values of **16** and **24** were estimated to be in the same range as **1** (Supporting Table S1), indicating that an electrostatic interaction may be required for potent inhibition of SIRT5 by mechanism-based inhibitors of this type. In addition, the substantial difference in potency between **23** and **24** indicates that both length and flexibility within the lysine side chain modification is important for high-affinity binding (Figure 1). During the course of these investigations, the laboratory of Jordan Meier has independently investigated the substitution of the carboxylic acid residue in ε-*N*-malonyllysine for a tetrazole moiety, to provide an isosteric element that does not undergo decarboxylation.[51] In that work, the modification was connected to lysine through a native amide bond to provide a substrate mimic that was recognized by both anti-Kmal antibody and SIRT5 enzyme. Because the native amide bond gives rise to a more flexible structure than the thioureas in our study and

4

because the malonyl analog is shorter than both the modifications in **23** and **24**, we think that these observations taken together further support that both distance and flexibility of the PTM are important for binding to SIRT5.

Finally, selectivity of the most potent inhibitors (**1**, **16**, **22**, and **24**) for SIRT5 over other members of the SIRT family was demonstrated using recombinant enzymes in vitro (Figure 1B; see Supporting Table S2 for IC_{50} values and additional examples).
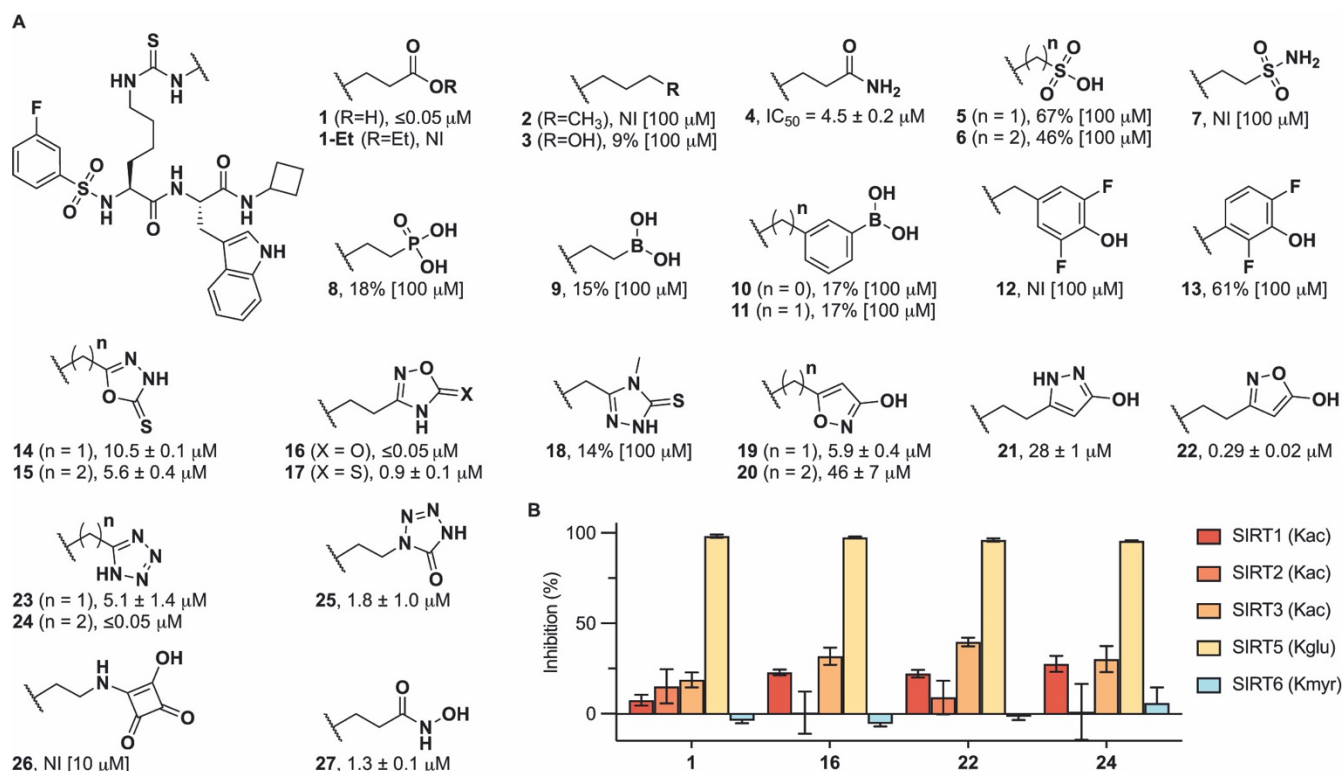
Figure 1. Structure-activity relationship of SIRT5 inhibitors containing carboxylic acid isosteres. (**A**) Potencies for inhibition of the deglutarylase activity of recombinant SIRT5 (150 nM) against Ac-LGKglut-AMC substrate (50 μM) are given as mean IC_{50} values ± standard deviation (SD) or %-inhibition at denoted concentrations. (**B**) Selectivity of compounds **1**, **16**, **22**, and **24** across SIRTs 1–3, 5, and 6 measured at an inhibitor concentration of 10 μM. The ε-N-acyllysine residue in each substrate is indicated for the individual sirtuin. Data are based on at least two individual assays performed in duplicate. See the Supporting Information Figure S1 for dose-response curves, Table S1 for inhibitory potencies, and Table S2 for full selectivity profiling.

Evaluation of inhibition kinetics. We have previously demonstrated that the use of IC_{50} values as the sole determination of potency can be misleading for mechanism-based sirtuin inhibitors, because these types of inhibitors may display time-dependent inhibition profiles.[44,52] Generally, SIRT inhibitors relying on a thiocarbonyl moiety are believed to gain their potency through formation of stalled intermediates with ADP-ribose from the NAD^+ co-substrate in the active sites of the enzymes. This mechanism, in turn, has been shown to result in slow, tight-binding inhibition kinetics rather than fast-on–fast-off kinetics, which is a prerequisite for estimating

K_i values by the Cheng-Prusoff equation. Furthermore, despite a relatively low K_M value for the applied substrate in our initial screen ($K_M = 20 \pm 1.9\ \mu$M, Supporting Figure S2 and Table S3), we noted that the most potent compounds had reached stoichiometric inhibition (*i.e.,* IC_{50} values in the same range as the enzyme concentration). Therefore, we turned to a continuous SIRT5 inhibition assay format that was previously used to determine the slow, tight-binding kinetics of compound **1**,[44] enabling more meaningful estimation of the potencies of compounds **16**, **22**, and **24**.
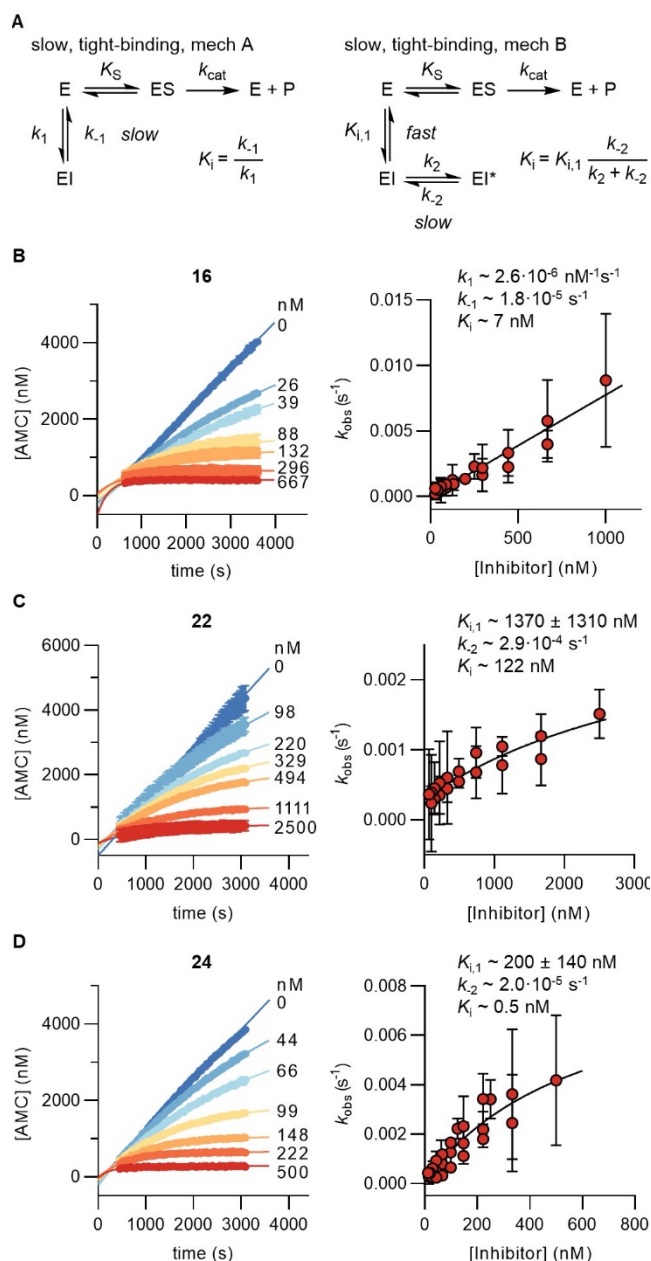
Figure 2. Kinetics of SIRT5 Inhibition by Compounds **16**, **22**, and **24**. (**A**) Common mechanisms of slow-binding inhibitor kinetics with associated equilibrium and rate constants. (**B**–**D**) Sample rate experiment curves and plots showing the dependence of k_{obs} on inhibitor concentration for compound **16** (mechanism A) as well as compounds **22** and **24** (mechanism B). Concentrations of inhibitor for each experiment indicated on the right side of the curve. Continuous assays were performed

with SIRT5 (80 nM), NAD$^+$ (500 μM), Ac-LGKglu-AMC (40 μM) as substrate, trypsin (1.70 ng μL^{-1}). See Supporting Figure S3 and Table S4 for additional details and complete data fitting.

Compounds **22** and **24** behaved as slow, tight-binding inhibitors like parent carboxylic acid-containing compound **1**, with K_i values in the low nanomolar range for both **1** and **24** and somewhat higher at around 100 nM for compound **22** (Figure 2 and Supporting Figure S3). The oxadiazolone-containing analog **16** exhibited slow-binding kinetics according to mechanism A, also with a K_i value in the low nanomolar range (Figure 2). The less potent analogs **4** and **27** were also evaluated in the continuous assay and displayed fast-on–fast-off kinetics with K_i values in the micromolar range. Their potencies, on the other hand, were in good agreement with the IC$_{50}$ values determined by end-point assays, as would be expected (Supporting Figure S3). Taken together, these assays show that the simple IC$_{50}$ determinations from end-point assays were useful as a screening platform but did not provide accurate affinities for the more potent compounds that exhibit longer residence times in the enzyme active site.

Evaluation in chloroalkane penetration assay (CAPA). Next, we proceeded to evaluate the effect of the bioisosteres on the overall ability to penetrate the cellular plasma membrane. We decided to apply the recently described chloroalkane penetration assay (CAPA).[50] Previous SAR studies have shown that the N-terminal functionality of the inhibitor scaffold can be substituted relatively flexibly without significant loss of potency.[44] We therefore attached the chloroalkane (CA) tag at the N-terminal through an amide linkage. Compounds **28**, **28-Et**, **29**–**31** were synthesized (Supporting Schemes S14 and S15) and their ability to enter cells in culture was analyzed in a HaloTag-expressing HeLa cell line (Figure 3). The cell penetration profiles of the CA-tagged compounds were analyzed by fitting as sigmoidal curves to the dose–response data. The concentration at which 50% cell penetration occurs is termed the CP$_{50}$ value, which we use to compare the cell penetrating properties fo the compounds. As positive control compound, we used tryptophan α-*N*-acylated with the same chloroalkane (**CA-Trp-OH**) to benchmark the degree of penetration of our compounds (Figure 3B and 3C).

The prodrug **28-Et** exhibited cell penetration ability with a CP$_{50}$ value in the same range as the control compound, while all the isosteric compounds tested (**29**–**31**) showed the same degree of penetration as the parent carboxylic acid (**1**). That **28-Et** reaches the intracellular matrix more readíly than **1** is in agreement with previously published data, showing cytotoxic effect of the prodrug but not the free carboxylic acid-containing compound (**1**) against SIRT5-dependent AML cell lines.[41] Unfortunately, however, all the isosteric compounds that showed high potency in enzymatic assays were exhibiting poor cell penetration with CP$_{50}$ values in the same range as the parent carboxylic acid (**1**) (Figure 3). We attribute this finding to the presumed negative charge in the side chains of all these analogs that would be expected in neutral medium based on their predicted pK_a values (Supporting Table S1). This assumption is further supported by the CP$_{50}$ values of additional compounds, showing high cell penetration with a simple alkyl side chain and poor cell penetration for additional negatively charged analogs (Supporting Figure S4).

Because the chloroalkane analogs **28–31** showed almost 10-fold higher CP_{50} values than the prodrug **32**, and because our SAR had suggested that an electrostatic interaction between ligand and SIRT5 active site was preferred for high affinity binding, we decided to prepare a compound containing a masked tetrazole functionality. Thus, an analog of compound **24**, containing an *O*-acyl-*N,O*-isobutyl hemiaminal functionality on the tetrazole moiety (**32**) was prepared (Figure 4 and Supporting Scheme S16). This functional group was chosen based on previous reports, showing improvement of cell penetration upon masking of tetrazoles using this chemistry.[53,54] Compound **32** would then presumably be cleaved by intracellular esterases to generate a readily hydrolyzed hemiaminal species that would provide the parent tetrazole **24**.
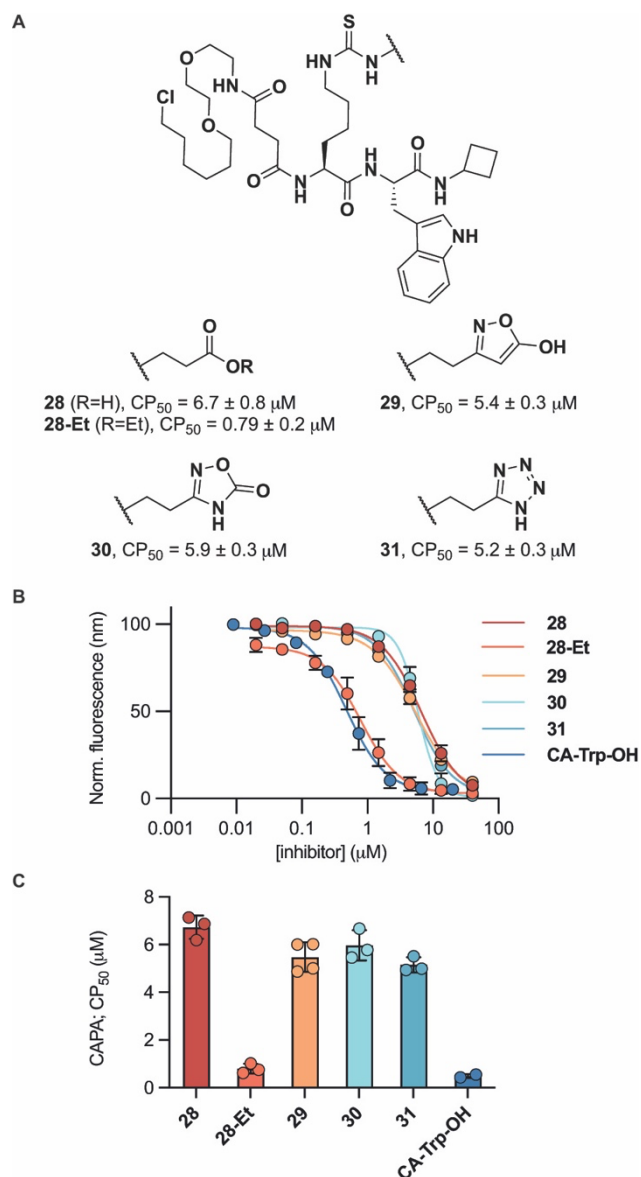
Figure 3. Cell penetration profiling using the CAPA assay. (**A**) Structure of synthesized chloroalkane probes and their mean CP_{50} values $\pm$ SD (n = 3). (**B**) CAPA results for compounds **28–31** and α-*N*-"chloroalkane"tryptophan **CA-Trp-OH** as the positive control after 4 hours of treatment with inhibitor (n $\geq$ 2). (**C**) Calculated CP_{50} values.
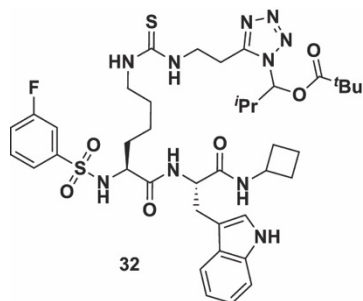
Figure 4. Structure of compound **32**.

Activity of compounds in cells. With compound **32** included in our collection, we next turned our attention to investigating the ability of selected compounds to reach the SIRT5 target in cultured cells. First, we chose immunoblot-based cellular thermal shift assays,[55,56] which we have previously applied for the investigation of engagement of mechanism-based inhibitors with SIRT1–3 in cells.[52,57] We decided to evaluate the thermal stabilization of the inhibitor–SIRT5 complex in HEK293T cells by determining isothermal dose–response cellular thermal shift curves ("ITDRF-CETSA").[56] The experiments were performed at 52 °C where most of the SIRT5 has denatured according to Western blot analysis (Supporting Figure S5). In the assays, two compounds (**16** and **22**) showed substantially lower degree of target engagement than the other tested analogs with EC_{50} values above the highest applied dose (>10 μM) (Figure 5). The parent compound **1** and tetrazole-containing analog **24** behaved similarly with EC_{50} values of 0.9 and 1.3 μM, respectively (Figure 5C). This agrees well with the findings that the two compounds have K_i values for inhibition of recombinant SIRT5 in the same range (Figure 2 and Supporting Figure S3) and their chloroalkane-tagged analogs exhibited similar cell penetrating profiles (Figure 3). Finally, the two compounds containing masked acidic functional groups (**1-Et** and **32**) also showed similar ability to engage SIRT5 in the cultured cells and to a higher extent than their unmasked counterparts (Figure 5). This, again, is in agreement with the data recorded for their chloroalkane-tagged analogs above and, further, indicates that both acidic functional groups are released within the cells to bind to the SIRT5 active site.

Next, we applied a recently developed assay that reports on SIRT5 enzymatic activity in the mitochondria by evaluating the fluorescence development caused by self-assembly of a dye-labeled peptide upon desuccinylation by SIRT5.[58] In this assay, we saw inhibition of SIRT5 activity for co-treatment of HeLa cells with the labeled peptide substrate and compounds **1-Et**, **24**, or **32** dosed at 10 μM concentration (Supporting Figure S6). The relatively high concentration of the inhibitors applied is likely the reason why we observe an effect of compound **24** as well as the masked compounds (**1-Et** and **32**), which exhibited superior levels of cell penetration and target engagement. However, we do not consider this assay sensitive enough to evaluate compound efficacies. Rather, we find it useful to investigate whether target engagement results in inhibition of the enzymatic activity in living cells as well. Therefore, we decided not to perform dose-response experiments using this assay.
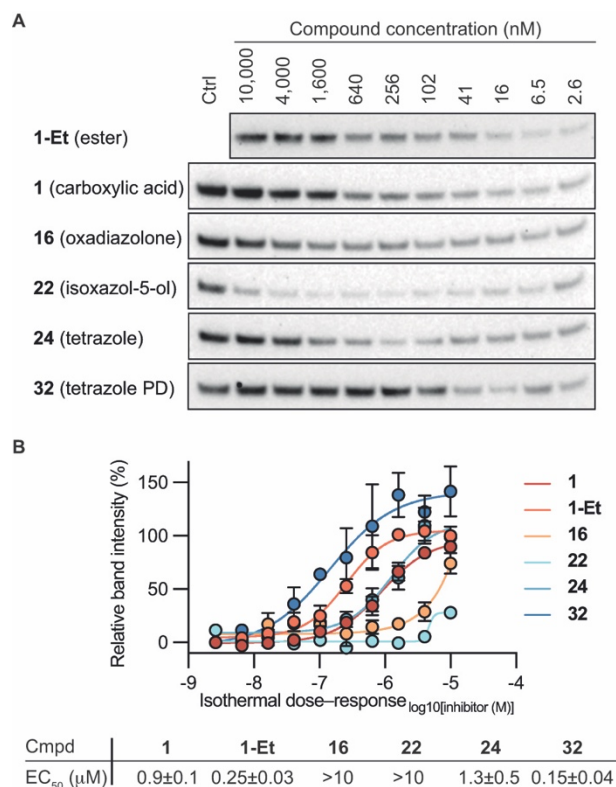
Figure 5. Cellular target engagement. Thermal shift of SIRT5 in HEK293T cells subjected to 2 h treatment with inhibitor at concentrations varying from 2.6 nM to 10 μM and **1-Et** (10 μM) as internal control at 52 °C. (**A**) Representative immunoblots of SIRT5. (**B**) Fitting of dose–response curves and calculated EC_{50} values. See the Supporting Information for full immunoblots (n $\geq$ 2).

Growth inhibtion. Finally, we evaluated a selection of compounds for their ability to decrease the viability of SIRT5-dependent SKM-1 AML cells versus non-malignant, immortalized HEK293T cells in culture. None of the acidic compounds **1**, **16**, and **24** caused substantial decrease in viability of any of the two cell lines at concentrations up to 100 μM (Figure 6). The masked compounds, on the other hand, exhibited GI_{50} values against SKM-1 cells of 21 μM (**1-Et**) and 9 μM (**32**), respectively. Inhibition of the growth of two additional SIRT5-dependent AML cell lines, OCI-AML2 and MOLM-13, by **1-Et** and **32** was then tested, which also showed more potent effect of the masked tetrazole (**32**) than **1-Et**. Moreover, the effect on HEK293T cells was minimal for **32** with <35% inhibition at 100 μM, indicating cytoselective toxicity towards SIRT5-selective cells to a substantially higher extent than for compound **1-Et** (Figure 6).
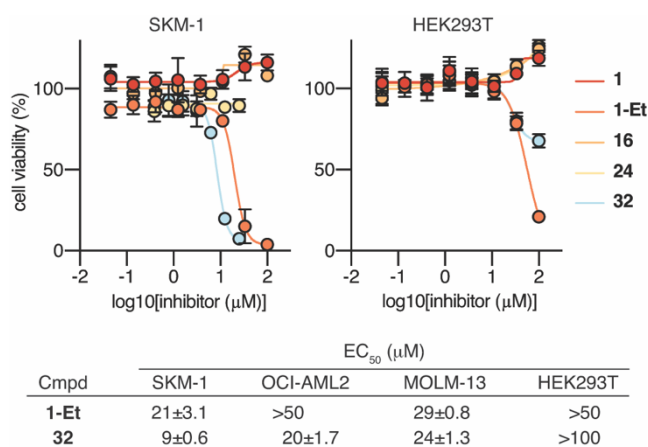
Figure 6. Cell viability upon treatment with **1, 1-Et, 16, 24**, and **32**. (**A**) Dose-response curves from cell viability assays of the selected compounds against cultured SKM-1 (SIRT5-dependent acute myeloid leukemia) cells and HEK293T (immortalized, non-malignant human embryonic kidney) cells as well as GI_{50} values of **1-Et** and **32** against OCI-AML2, MOLM-13 (SIRT5-dependent acute myeloid leukemia) cells. All values represent data from three individual assays performed in duplicate (see the Supporting Information Figure S7 for additional dose-response curves).

Discussion

We have investigated the prospects of substituting the carboxylic acid moiety, which provides both potency and selectivity to mechanism-based inhibitors of SIRT5, by isosteric functional groups. In the initial SAR study, we prepared 25 different compounds with a variety of substituents that were envisioned to interact with the Tyr102–Arg105 motif in the active site of SIRT5 and tested them all for their ability to inhibit the enzymatic activity of recombinant SIRT5 in vitro. This investigation indicated that introduction of the tetrazole (**24**) and the 1,2,4-oxadiazol-5(4*H*)-one (**16**) in place of the parent carboxylate (**1**) resulted in similar affinity for the enzyme. Because the compounds were potent enough to reach stoichiometry with respect to the amount of enzyme applied in the assay, we performed a kinetic enzyme inhibition experiment, using continuous assays to provide progress curves for the inhibition over time. Analysis of these data revealed these potent compounds inhibit SIRT5 through slow, tight-binding kinetics with estimated K_i values ranging from ~0.5–7 nM, where the tetrazole-containing compound is the most potent.

Encouraged by the discovery of compounds containing isosteres that potently bind to the enzyme, we next evaluated the ability of a subset of compound scaffolds to reach the intracellular matrix of HeLa cells in culture. The so-called CAPA method was applied to compare selected scaffolds by measuring the ability of chloroalkane-modified versions to enter engineered HeLa cells that express the HaloTag enzyme. The resulting data showed a substantially lower cell penetration of the carboxylic acid parent compound and its most potent heterocyclic isosteres than the chloroalkane analog of the ester prodrug, previously also shown to exhibit activity against

SIRT5-dependent AML cells (compound **1-Et**). This result led us to design and synthesize a masked version of the tetrazole-containing compound (**32**), which was included in the following compound evaluations.

Isothermal dose–response cellular target engagement experiments in HEK293T cells showed substantially lower EC_{50} values for the masked compounds compared to their unmasked counterparts [**1-Et** vs **1** (3.6-fold) and **32** vs **24** (8.7-fold)]. Both compounds were also shown to inhibit SIRT5 in HeLa cells by using an assay that produce in cell fluoresence in response to SIRT5 activity in the mitochondria. Finally, the two masked compounds were shown to harbor cytoselective toxicity towards SIRT5-dependent AML cells (SKM-1) over HEK293T cells in culture, while none of the the unmasked compounds tested were able to affect the cell viability in either cell line at the highest concentration applied.

In summary, our SAR demonstrated that size, orientation, hydrogen bonding properties, and charge of the bioisosteres were important for retaining affinity by interaction with the Tyr102–Arg105 motif in the active site of SIRT5. The most promising chemotypes in our series of inhibitors had pK_a values in the same range as the parent carboxylate, which appeared to hamper cell penetration and, in turn, needed to be further masked to provide an inhibitor with activity in cells. We therefore designed a masked tetrazole-containing compound, which exhibited more potent and selective cytotoxic effect against SIRT5-dependent AML cell lines than the previously developed ester prodrugs of carboxylic acids. Thus, these data provide insight into future inhibitor design principles and expand the functionalities that can be used to inhibit SIRT5. Further, we expect the developed inhibitor to enable more detailed investigation of the biology of SIRT5 and help illuminate its potential as a target for pharmacological intervention in cancer treatment. It is our hope that the insight gained from this study will inspire the exploration of new avenues in the pursuit of drug discovery efforts targeting sirtuin enzymes.

Conflict of Interest

The authors declare no competing financial interest(s)

Supporting Information

Supporting Schemes, Figures, and Tables, general methods and materials, biochemical methods, supporting references, as well as copies ^{1}H and ^{13}C NMR spectra (PDF)

ORCID

Nima Rajabi: 0000-0002-9509-7540

Alexander L. Nielsen: 0000-0003-1195-0143

Tobias N. Hansen: 0000-0001-6098-058X

Huy Nguyen: 0000-0001-8962-9291

Michael Bæk: 0000-0001-7416-9421

Julie E. Bolding: 0000-0003-2735-2519

Christian R. Bartling: 0000-0002-0602-4738

Kristian Strømgaard: 0000-0003-2206-4737

Christian A. Olsen: 0000-0002-2953-8942

References

[1] S. Michan, D. Sinclair, *Biochem. J.* **2007**, *404*, 1–13.

[2] R. H. Houtkooper, E. Pirinen, J. Auwerx, *Nat. Rev. Mol. Cell. Biol.* **2012**, *13*, 225–238.

[3] P. Bheda, H. Jing, C. Wolberger, H. Lin, *Annu. Rev. Biochem.* **2016**, *85*, 405–429.

[4] B. R. Sabari, D. Zhang, C. D. Allis, Y. Zhao, *Nat. Rev. Mol. Cell. Biol.* **2017**, *18*, 90–101.

[5] N. Rajabi, I. Galleano, A. S. Madsen, C. A. Olsen, in *Prog. Mol. Biol .Transl. Sci.*, Academic Press, **2018**, pp. 25–69.

[6] M. Wang, H. Lin, *Annu. Rev. Biochem.* **2021**, *90*, 245–285.

[7] J. L. Feldman, J. Baeza, J. M. Denu, *J. Biol. Chem.* **2013**, *288*, 31350–31356.

[8] A. S. Madsen, C. Andersen, M. Daoud, K. A. Anderson, J. S. Laursen, S. Chakladar, F. K. Huynh, A. R. Colaço, D. S. Backos, P. Fristrup, M. D. Hirschey, C. A. Olsen, *J. Biol. Chem.* **2016**, *291*, 7128–7141.

[9] M. A. Klein, C. Liu, V. I. Kuznetsov, J. B. Feltenberger, W. Tang, J. M. Denu, *J. Biol. Chem.* **2020**, *295*, 1385–1399.

[10] L. Jin, W. Wei, Y. Jiang, H. Peng, J. Cai, C. Mao, H. Dai, W. Choy, J. E. Bemis, M. R. Jirousek, J. C. Milne, C. H. Westphal, R. B. Perni, *J. Biol. Chem.* **2009**, *284*, 24394–24405.

[11] H. Jiang, S. Khan, Y. Wang, G. Charron, B. He, C. Sebastian, J. Du, R. Kim, E. Ge, R. Mostoslavsky, H. C. Hang, Q. Hao, H. Lin, *Nature* **2013**, *496*, 110–113.

[12] Y. Bin Teng, H. Jing, P. Aramsangtienchai, B. He, S. Khan, J. Hu, H. Lin, Q. Hao, *Sci. Rep.* **2014**, *5*, 8529.

[13] A. M. Davenport, F. M. Huber, A. Hoelz, *J. Mol. Biol.* **2014**, *426*, 526–541.

[14] D. O. Gaffney, E. Q. Jennings, C. C. Anderson, J. O. Marentette, T. Shi, A. M. Schou Oxvig, M. D. Streeter, M. Johannsen, D. A. Spiegel, E. Chapman, J. R. Roede, J. J. Galligan, *Cell Chem. Biol.* **2020**, *27*, 206-213.e6.

[15] C. Moreno-Yruela, D. Zhang, M. Bæk, W. Wei, J. Gao, A. L. Nielsen, J. B. Bolding, S. T. Jameson, C. A. Olsen, Y. Zhao, *bioRxiv* **2021**, DOI 10.1101/2021.03.24.436780.

[16] K. A. Anderson, F. K. Huynh, K. Fisher-Wellman, J. D. Stuart, B. S. Peterson, J. D. Douros, G. R. Wagner, J. W. Thompson, A. S. Madsen, M. F. Green, R. M. Sivley, O. R. Ilkayeva, R. D. Stevens, D. S. Backos, J. A. Capra, C. A. Olsen, J. E. Campbell, D. M. Muoio, P. A. Grimsrud, M. D. Hirschey, *Cell Metab.* **2017**, *25*, 838–855.

[17] M. Pannek, Z. Simic, M. Fuszard, M. Meleshin, D. Rotili, A. Mai, M. Schutkowski, C. Steegborn, *Nat.*

Commun. **2017**, *8*, 1513.

[18]   R. A. A. Mathias, T. M. M. Greco, A. Oberstein, H. G. G. Budayeva, R. Chakrabarti, E. A. A. Rowland, Y. Kang, T. Shenk, I. M. M. Cristea, *Cell* **2014**, *159*, 1615–1625.

[19]   Z. Tong, M. Wang, Y. Wang, D. D. Kim, J. K. Grenier, J. Cao, S. Sadhukhan, Q. Hao, H. Lin, *ACS Chem. Biol.* **2017**, *12*, 300–310.

[20]   M. Tang, Z. Li, C. Zhang, X. Lu, B. Tu, Z. Cao, Y. Li, Y. Chen, L. Jiang, H. Wang, L. Wang, J. Wang, B. Liu, X. Xu, H. Wang, W. G. Zhu, *Sci. Adv.* **2019**, *5*, eaav1118.

[21]   X. Bao, Z. Liu, W. Zhang, K. Gladysz, Y. M. E. Fung, G. Tian, Y. Xiong, J. W. H. Wong, K. W. Y. Yuen, X. D. Li, *Mol. Cell* **2019**, *76*, 660–675.

[22]   Z. Tong, Y. Wang, X. Zhang, D. D. Kim, S. Sadhukhan, Q. Hao, H. Lin, *ACS Chem. Biol.* **2016**, *11*, 742–747.

[23]   C. Peng, Z. Lu, Z. Xie, Z. Cheng, Y. Chen, M. Tan, H. Luo, Y. Zhang, W. He, K. Yang, B. M. M. Zwaans, D. Tishkoff, L. Ho, D. Lombard, T. C. He, J. Dai, E. Verdin, Y. Ye, Y. Zhao, *Mol. Cell. Proteomics* **2011**, *10*, DOI 10.1074/mcp.M111.012658.

[24]   J. Du, Y. Zhou, X. Su, J. J. Yu, S. Khan, H. Jiang, J. Kim, J. Woo, J. H. Kim, B. H. Choi, B. He, W. Chen, S. Zhang, R. A. Cerione, J. Auwerx, Q. Hao, H. Lin, *Science* **2011**, *334*, 806–809.

[25]   M. Tan, C. Peng, K. A. Anderson, P. Chhoy, Z. Xie, L. Dai, J. Park, Y. Chen, H. Huang, Y. Zhang, J. Ro, G. R. Wagner, M. F. Green, A. S. Madsen, J. Schmiesing, B. S. Peterson, G. Xu, O. R. Ilkayeva, M. J. Muehlbauer, T. Braulke, C. Mühlhausen, D. S. Backos, C. A. Olsen, P. J. McGuire, S. D. Pletcher, D. B. Lombard, M. D. Hirschey, Y. Zhao, *Cell Metab.* **2014**, *19*, 605–617.

[26]   J. Park, Y. Chen, D. X. Tishkoff, C. Peng, M. Tan, L. Dai, Z. Xie, Y. Zhang, B. M. M. Zwaans, M. E. Skinner, D. B. Lombard, Y. Zhao, *Mol. Cell* **2013**, *50*, 919–930.

[27]   M. J. Rardin, W. He, Y. Nishida, J. C. Newman, C. Carrico, S. R. Danielson, A. Guo, P. Gut, A. K. Sahu, B. Li, R. Uppala, M. Fitch, T. Riiff, L. Zhu, J. Zhou, D. Mulhern, R. D. Stevens, O. R. Ilkayeva, C. B. Newgard, M. P. Jacobson, M. Hellerstein, E. S. Goetzman, B. W. Gibson, E. Verdin, *Cell Metab.* **2013**, *18*, 920–933.

[28]   Y. Nishida, M. J. Rardin, C. Carrico, W. He, A. K. Sahu, P. Gut, R. Najjar, M. Fitch, M. Hellerstein, B. W. Gibson, E. Verdin, *Mol. Cell* **2015**, *59*, 321–332.

[29]   Z. F. Lin, H. B. Xu, J. Y. Wang, Q. Lin, Z. Ruan, F. B. Liu, W. Jin, H. H. Huang, X. Chen, *Biochem. Biophys. Res. Commun.* **2013**, *441*, 191–195.

[30]   H. Guedouari, T. Daigle, L. Scorrano, E. Hebert-Chatelain, *Biochim. Biophys. Acta - Mol. Cell Res.* **2017**,

1864, 169–176.

[31]   F. Wang, K. Wang, W. Xu, S. Zhao, D. Ye, Y. Wang, Y. Xu, L. Zhou, Y. Chu, C. Zhang, X. Qin, P. Yang, H. Yu, *Cell Rep.* **2017**, *19*, 2331–2344.

[32]   W. Lu, Y. Zuo, Y. Feng, M. Zhang, *Tumor Biol.* **2014**, *35*, 10699–10705.

[33]   X. Ye, X. Niu, L. Gu, Y. Xu, Z. Li, Y. Yu, Z. Chen, S. Lu, *Oncotarget* **2017**, *8*, 6984–6993.

[34]   Y. Q. Wang, H. L. Wang, J. Xu, J. Tan, L. N. Fu, J. L. Wang, T. H. Zou, D. F. Sun, Q. Y. Gao, Y. X. Chen, J. Y. Fang, *Nat. Commun.* **2018**, *9*, 545.

[35]   L. Chang, L. Xi, Y. Liu, R. Liu, Z. Wu, Z. Jian, *Mol. Med. Rep.* **2018**, *17*, 342–349.

[36]   S. Kumar, D. B. Lombard, *Crit. Rev. Biochem. Mol. Biol.* **2018**, *53*, 311–334.

[37]   L. Xu, X. Che, Y. Wu, N. Song, S. Shi, Sh. O. Wang, C. Li, Lingy. N. Zhang, X. Zhang, Xi. A. Qu, Y. E. Teng, *Oncol. Rep.* **2018**, *39*, 2315–2323.

[38]   X. Yang, Z. Wang, X. Li, B. Liu, M. Liu, L. Liu, S. Chen, M. Ren, Y. Wang, M. Yu, B. Wang, J. Zou, W. G. Zhu, Y. Yin, W. Gu, J. Luo, *Cancer Res.* **2018**, *78*, 372–386.

[39]   X. Sun, S. Wang, J. Gai, J. Guan, J. Li, Y. Li, J. Zhao, C. Zhao, L. Fu, Q. Li, *Front. Oncol.* **2019**, *9*, 754.

[40]   Y. L. N. Abril, I. R. Fernandez, J. Y. Hong, Y. L. Chiang, D. A. Kutateladze, Q. Zhao, M. Yang, J. Hu, S. Sadhukhan, B. Li, B. He, B. Remick, J. J. Bai, J. Mullmann, F. Wang, V. Maymi, R. Dhawan, J. Auwerx, T. Southard, R. A. Cerione, H. Lin, R. S. Weiss, *Oncogene* **2021**, *40*, 1644–1658.

[41]   D. Yan, A. Franzini, A. D. Pomicter, B. J. Halverson, O. Antelope, C. C. Mason, J. M. Ahmann, A. V. Senina, N. A. Vellore, C. L. Jones, M. S. Zabriskie, H. Than, M. J. Xiao, A. van Scoyk, A. B. Patel, P. M. Clair, W. L. Heaton, S. C. Owen, J. L. Andersen, C. M. Egbert, J. A. Reisz, A. D'Alessandro, J. E. Cox, K. C. Gantz, H. M. Redwine, S. M. Iyer, J. S. Khorashad, N. Rajabi, C. A. Olsen, T. O'Hare, M. W. Deininger, *Blood Cancer Discov.* **2021**, *2*, 266–287.

[42]   A. S. Madsen, C. A. Olsen, *J. Med. Chem.* **2012**, *55*, 5582–5590.

[43]   C. Roessler, T. Nowak, M. Pannek, M. Gertz, G. T. T. Nguyen, M. Scharfe, I. Born, W. Sippl, C. Steegborn, M. Schutkowski, *Angew. Chem. Int. Ed.* **2014**, *53*, 10728–10732.

[44]   N. Rajabi, M. Auth, K. R. Troelsen, M. Pannek, D. P. Bhatt, M. Fontenas, M. D. Hirschey, C. Steegborn, A. S. Madsen, C. A. Olsen, *Angew. Chem. Int. Ed.* **2017**, *56*, 14836–14841.

[45]   B. He, J. Du, H. Lin, *J. Am. Chem. Soc.* **2012**, *134*, 1922–1925.

[46]   H. Lin, R. Cerione, *(Cornell University), Methods for Treatment of Cancer by Targeting SIRT5. US 2014213530 A1, Jul 31, 2014.*, **n.d.**, US2014197775.

[47] W. Zang, Y. Hao, Z. Wang, W. Zheng, *Bioorganic Med. Chem. Lett.* **2015**, *25*, 3319–3324.

[48] L. Polletta, E. Vernucci, I. Carnevale, T. Arcangeli, D. Rotili, S. Palmerio, C. Steegborn, T. Nowak, M. Schutkowski, L. Pellegrini, L. Sansone, L. Villanova, A. Runci, B. Pucci, E. Morgante, M. Fini, A. Mai, M. A. Russo, M. Tafani, *Autophagy* **2015**, *11*, 253–270.

[49] L. Peraro, Z. Zou, K. M. Makwana, A. E. Cummings, H. L. Ball, H. Yu, Y.-S. Lin, B. Levine, J. A. Kritzer, *J. Am. Chem. Soc.* **2017**, *139*, 7792–7802.

[50] L. Peraro, K. L. Deprey, M. K. Moser, Z. Zou, H. L. Ball, B. Levine, J. A. Kritzer, *J. Am. Chem. Soc.* **2018**, *140*, 11360–11369.

[51] Y. Jing, S. E. Bergholtz, A. Omole, R. A. Kulkarni, T. T. Zengeya, E. Yoo, J. L. Meier, *ChemBioChem* **2021**, 2020.08.23.263285.

[52] A. L. Nielsen, N. Rajabi, N. Kudo, K. Lundø, C. Moreno-Yruela, M. Bæk, M. Fontenas, A. Lucidi, A. S. Madsen, M. Yoshida, C. A. Olsen, *RSC Chem. Biol.* **2021**, *2*, 612–626.

[53] D. E. Ryono, J. Lloyd, M. A. Poss, J. E. Bird, J. Buote, S. Chong, T. Dejneka, K. E. J. Dickinson, Z. Gu, P. Mathers, S. Moreland, R. A. Morrison, E. W. Petrillo, J. R. Powell, T. Schaeffer, E. R. Spitzmiller, R. E. White, *Bioorganic Med. Chem. Lett.* **1994**, *4*, 201–206.

[54] N. J. O'Brien, S. Amran, J. Medan, B. Cleary, L. W. Deady, I. G. Jennings, P. E. Thompson, B. M. Abbott, *ChemMedChem* **2013**, *8*, 914–918.

[55] D. M. Molina, R. Jafari, M. Ignatushchenko, T. Seki, E. A. Larsson, C. Dan, L. Sreekumar, Y. Cao, P. Nordlund, D. Martinez Molina, R. Jafari, M. Ignatushchenko, T. Seki, E. A. Larsson, C. Dan, L. Sreekumar, Y. Cao, P. Nordlund, *Science* **2013**, *341*, 84–87.

[56] R. Jafari, H. Almqvist, H. Axelsson, M. Ignatushchenko, T. Lundbäck, P. Nordlund, D. M. Molina, *Nat. Protoc.* **2014**, *9*, 2100–2122.

[57] K. S. Troelsen, M. Bæk, A. L. Nielsen, A. S. Madsen, N. Rajabi, C. A. Olsen, *RSC Chem. Biol.* **2021**, *2*, 627–635.

[58] L. Yang, R. Peltier, M. Zhang, D. Song, H. Huang, G. Chen, Y. Chen, F. Zhou, Q. Hao, L. Bian, M. He, Z. Wang, Y. Hu, H. Sun, *J. Am. Chem. Soc.* **2020**, *142*, 18150–18159.